


ORIGINAL ARTICLE

Soluble *Vegfr3* gene therapy suppresses multi-organ metastasis in a mouse mammary cancer modelMasa-Aki Shibata¹  | Eiko Shibata² | Yoshihisa Tanaka¹ | Chinatsu Shiraoka¹ | Yoichi Kondo¹¹Department of Anatomy and Cell Biology, Osaka Medical College, Takatsuki, Japan²Department of Molecular Innovation in Lipidology, National Cerebral & Cardiovascular Center Research Institute, Suita, Japan**Correspondence**Masa-Aki Shibata, Department of Anatomy and Cell Biology, Osaka Medical College, 2-7 Daigaku-machi, Takatsuki, Osaka 569-8686, Japan.
Email: an1031@osaka-med.ac.jp**Funding information**

Ministry of Education, Culture, Sports, Science and Technology of Japan, Grant/Award Number: 21591682

Abstract

Accumulating evidence on the association of VEGF-C with lymphangiogenesis and lymph node metastasis implicates lymphatic vessels as a potential target in anti-cancer therapy. To evaluate whether blocking VEGF-C and VEGFR-3 signaling can inhibit multi-organ metastases, a mouse metastatic mammary cancer model was subjected to gene therapy using a soluble VEGFR-3 expression vector (psVEGFR-3). We showed that psVEGFR-3 significantly diminished cell growth in vitro with or without added VEGF-C, and significantly reduced primary tumor growth and tumor metastases to wide-spectrum organs in vivo. Although apoptotic cell death and angiogenesis levels did not differ between the control and psVEGFR-3 groups, cell proliferation and lymphangiogenesis in the mammary tumors were significantly decreased in the psVEGFR-3 group. Furthermore, lymphatic vessel invasion was significantly inhibited in this group. Real-time RT-PCR analysis revealed significantly high expression of the *Vegfr3* gene due to gene therapy, and the transcriptional levels of *Pcna* and *Lyve1* tended to decrease in the psVEGFR-3 group. Immunofluorescence staining indicated that phospho-tyrosine expression was considerably lower in tumor cells of psVEGFR-3-treated mammary carcinomas than those of control tumors. Double immunofluorescence staining indicated that phospho-tyrosine⁺/LYVE-1⁺ (a lymphatic vessel marker) tended to decrease in psVEGFR-3-treated mammary carcinomas compared with control mice, indicating a decline in the activity of the VEGF-C/VEGFR-3 axis. These findings showed that a blockade of VEGF-C/VEGFR-3 signaling caused by sVEGFR-3 sequestered VEGF-C and prevented the side-effects of anti-angiogenesis and suppressed overall metastases, suggesting their high clinical significance.

KEYWORDS

anti-metastasis, antitumor, mammary cancer, multi-organ metastasis, soluble VEGFR-3

Abbreviations: *bla*^R, blastidicin resistance gene; FPPE, formalin-fixed paraffin-embedded; *Lyve1*, lymphatic vessel endothelial hyaluronan receptor 1; PCNA, proliferating cell nuclear antigen; psVEGFR-3, soluble vascular endothelial growth factor receptor-3 expression vector; p-Tyr, phospho-tyrosine; pVec, empty plasmid vector; siRNA, small interfering RNA; sVEGFR, soluble vascular endothelial growth factor receptor; TUNEL, terminal deoxynucleotidyl transferase dUTP nick end labeling; VEGF, vascular endothelial growth factor; VEGFR, vascular endothelial growth factor receptor.

This is an open access article under the terms of the Creative Commons Attribution-NonCommercial License, which permits use, distribution and reproduction in any medium, provided the original work is properly cited and is not used for commercial purposes.

© 2020 The Authors. *Cancer Science* published by John Wiley & Sons Australia, Ltd on behalf of Japanese Cancer Association.

1 | INTRODUCTION

Cancer fact sheets from the World Health Organization show that cancer is a leading cause of death worldwide, accounting for an estimated 9.6 million deaths in 2018; that is, approximately 1 in 6 deaths are attributed to cancer.¹ Breast cancer is the second-most prevalent type of cancer worldwide in women of all ages and was ranked fifth as the cause of overall cancer mortality in 2018, when an estimated 2.09 million new cases corresponded to 22% of all cancers reported globally.¹ The increasing incidence of breast cancer among women under 40 y of age^{2,3} is of significant concern. As the lethality of breast cancer is attributed to its high propensity for metastasis to the lymph nodes, lungs, and bones,⁴ anti-metastatic therapies are of paramount importance.

The VEGF family participates in developmental vasculogenesis, physiological angiogenesis/lymphangiogenesis, and associated pathological conditions.^{5,6} Members of the VEGF family promote the formation of new blood and lymphatic vessels in tumor tissues, enabling the spread of tumor cells.⁷ Within the VEGF family, VEGF-C has been reported to induce lymphangiogenesis by activation of VEGFR-3 (VEGF-C receptor) that is expressed in lymphatic endothelial cells.^{8,9} VEGF-C has been reported to enhance lymphatic metastasis and is associated with lymphangiogenesis in animal models,¹⁰⁻¹³ while clinical studies indicate an association between VEGF-C overexpression in tumors with lymph node metastasis and poor prognosis in breast cancer patients.¹⁴⁻¹⁶

Blocking VEGFR-3 signaling using anti-VEGFR-3 antibody,^{17,18} small interfering RNA (siRNA),¹⁹⁻²² or soluble VEGFR-3 (sVEGFR-3)²³⁻²⁵ has been reported to suppress tumor lymphangiogenesis and lymph node metastasis in animal cancer models. sVEGFR-3 binds and sequesters VEGF-C, thereby blocking VEGFR-3-mediated signaling. In a previous study, we developed a mouse mammary cancer model that demonstrated metastasis of wide-spectrum organs,^{26,27} therefore, in the current study, we attempted the suppression of multi-organ metastasis by *sVegfr3* therapy in a mouse model of metastatic mammary cancer.

2 | MATERIALS AND METHODS

2.1 | Vectors

The *sVegfr3* (nucleotides 91-2413 from murine *Flt4* NM_008029) sequence and the *interleukin-2* signal sequence for secretion (pBLAST2-mFlt4 vector) were inserted into the pUNO1 expression vector (InvivoGen Inc.). The plasmid vector is regulated by the elongation factor-1 α /human T cell leukemia virus type 1 long terminal repeat hybrid promoter and includes *bla^R* (blasticidin resistance gene). To generate the empty control vector, the *sVegfr3* gene was deleted from the pBLAST2-mFlt4 vector by digestion with *Agel*/*NheI*. These vectors are referred to as psVEGFR-3 and pVec (control), respectively, in this study. The vectors were isolated from *Escherichia coli* (DH5 α strain) and purified by a modified alkaline

lysis procedure using an endotoxin-free Plasmid Maxi Kit (Qiagen, GmbH, Hilden, Germany) and further purified using centrifugal filters (Ultrafree-MC, Millipore).

2.2 | Cell line and animals

Mammary tumors arising from BJMC3879 cell implantation have a high metastatic predilection for the lymph nodes and lungs,^{20,28} a trait retained through culture. To monitor in vivo progression and dissemination, we conducted a stable transfection of the BJMC3879 parent cell line with *luc2* (improved *firefly luciferase* gene) and generated the BJMC3879Luc2 mammary carcinoma cell line.²⁹ Mammary carcinomas induced by BJMC3879Luc2 inoculation have a mutant p53 protein.²⁷ BJMC3879Luc2 cells used in this study were maintained in Dulbecco's modified Eagle's medium with 10% FBS and penicillin-streptomycin and grown at 37°C in an incubator containing 5% CO₂ in air.

Five-wk-old female BALB/c mice (n = 30) were purchased from Japan SLC, Inc. Five animals were housed per plastic cage on wood chip bedding with free access to water and food under controlled temperature (21 \pm 2°C), humidity (50 \pm 10%), and lighting (12 h : 12 h, light : dark cycle). All animal experiments were approved by the Institutional Review Board of the Osaka Medical College (approval no. 21051) and were performed according to procedures outlined in the Guide for the Animal Care and Use of Laboratory Animals of the Osaka Medical College.

2.3 | Study in vitro

We incubated BJMC3879Luc2 cells (1 \times 10⁴ cells) with mouse recombinant VEGF-C (0-200 ng/mL) in a 96-well plate in vitro to clarify the proliferative activity of VEGF-C on mammary carcinoma cells. Cell growth was determined after 24 h of VEGF-C addition using water-soluble tetrazolium (WST-1), as described by the manufacturer (TaKaRa Bio) and with use of a microplate reader (Bio-Rad). We then validated psVEGFR-3 vector function by transfecting BJMC3879Luc2 cells with psVEGFR-3 or pVec (control) using a Nucleofector (amaxa Biosystems GmbH) with or without VEGF-C addition (100 ng/mL). Cell growth was determined 48 h post-transfection as described above.

2.4 | Gene therapy with *sVegfr3* in vivo

We inoculated BJMC3879Luc2 cells (2.5 \times 10⁶ cells/0.3 ml in PBS) subcutaneously into the right inguinal region of 30 female BALB/c mice. At 2 wk post-inoculation, when the resulting tumors were 0.4-0.5 cm in diameter, the animals were allocated into 2 groups of 10 mice each (the psVEGFR-3 or control pVec groups) to prevent variations in tumor size. The 10 remaining mice were euthanized. Following this, we injected psVEGFR-3 or pVec (0.5 μ g/ μ L saline) directly into the tumors using a

27-gauge needle while the animals were under isoflurane anesthesia. In vivo gene electrotransfer was performed immediately afterwards by applying a conductive gel (Echo Jelly; Aloka Co., Ltd.) topically to the unshaved skin over the tumor and to the surface of small platinum 'forceps' electrode plates. Electric pulses were then delivered directly into the tumor via the plate electrodes (CUY650-10; Bex Co., Ltd.) using a CUY21EDIT square-wave electropulser (Bex Co., Ltd.) generating 8 pulses with a pulse length of 20 ms at 100 V.^{28,30} Vector injection and gene electrotransfer were performed once a week for 6 wk. As the tumors grew, a volume of $\leq 150 \mu\text{l}$ of vector solution was introduced into the larger masses, while smaller tumors that were 0.6–0.7 cm in diameter were infused until we detected leakage of the vector solution; approximately 50–75 μg of plasmid/tumor was administered, depending on tumor size.

Individual body weights were recorded weekly, along with measurement of each mammary tumor using digital calipers. Primary tumor volumes were then recorded based on the following formula: maximum diameter \times (minimum diameter)² \times 0.4.³¹

2.5 | Bioluminescence imaging in vivo

At experimental week 6, 6 mice from each group were anesthetized by isoflurane inhalation using an anesthesia system (SBH Designs Inc.). Each anesthetized mouse received an intraperitoneal injection of 3 mg D-luciferin potassium salt (Fujifilm Wako Pure Chemical Co.) in PBS prior to bioluminescence imaging using a Photon Imager (Biospace Lab). After 10 min, the mice were placed on a heated platform maintained at 37°C inside the Photon Imager. Photon emission was dynamically measured during acquisition for 5 min using the Photon Imager. An elliptical region of interest (ROI) was drawn over the tumor and metastatic locations for image analysis and total photon counts were calculated using Photovision software (Biospace Lab).

2.6 | Preparation for histopathological analyses

At necropsy (after week 6), we harvested the primary tumors and lymph nodes from the axillary and inguinal regions of all mice, along with any other lymph nodes that appeared abnormal, and fixed the tissues in 10% phosphate-buffered formalin solution. Lungs, kidneys, adrenals, ovaries, and other tissues/organs that appeared abnormal were routinely excised and immersed in the formalin solution for paraffin embedding. The lungs were inflated with the fixative before excision. All FFPE tissues were cut in sequential 4- μm sections for histopathological analysis using hematoxylin and eosin (H&E) and immunohistochemical staining.

2.7 | Immunohistochemistry

We conducted antigen retrieval (autoclaved for 10 min at 110°C) using a Tris-EDTA buffer (pH 9.0) for all immunohistochemical

staining procedures. The primary antibodies used were as follows: anti-PCNA rabbit polyclonal antibody (Proteintech Group, Inc.), anti-CD31 rabbit polyclonal antibody (Lab Vision), anti-podoplanin hamster monoclonal antibody (AngioBio Co.), and anti-LYVE-1 rabbit polyclonal antibody (Acris Antibodies GmbH). We incubated the slides with the corresponding biotinylated secondary antibodies using an established labeled streptavidin-biotin method (Dako Co.), with exposure to 3,3'-diaminobenzidine (DAB) and hematoxylin counterstain for visualizing the immunocomplexes formed.

Lymphangiogenesis is induced by VEGF-C via VEGFR-3 phosphorylation. The tyrosine kinase receptor for VEGF-C is VEGFR-3 and it is expressed in lymphatic endothelial cells.² However, as reliable antibodies against mouse phosphorylated VEGFR-3 are not commercially available, we double stained FFPE primary tumor sections with immunofluorescence using mouse monoclonal anti-phospho-tyrosine (p-Tyr; Santa Cruz Biotechnology Inc.) and rat monoclonal anti-LYVE-1 (Acris Antibodies GmbH) antibodies. Unstained sections underwent antigen retrieval as mentioned above prior to incubation with primary antibodies. The slides were exposed to secondary antibodies anti-mouse Alexa Fluor 594 (for p-Tyr) and anti-rat Alexa Fluor 488 (for LYVE-1) (Molecular Probes) with nuclear staining by mounting in medium containing DAPI (Vector Laboratories). LYVE-1⁺ or p-Tyr⁺/LYVE-1⁺ was quantified and expressed as number per cm² tumor area.

2.8 | Apoptosis and cell proliferation

We examined FFPE primary tumor sections for quantitative analyses of apoptotic cell death using TUNEL staining (Fujifilm Wako Pure Chemical Co.). TUNEL-positive cells were enumerated only in viable tumor regions peripheral to the central necrotic areas. We counted TUNEL-positive cells in each of 4 randomly selected microscopic fields ($\sim 130\,000 \mu\text{m}^2/\text{field}$) of viable tissue at $\times 200$ magnification. The results are expressed as numbers of TUNEL-positive cells per cm².

Primary mammary tumors were evaluated for cell proliferation as determined by PCNA-positive nuclear staining. We counted the numbers of PCNA-positive cells in each of 4 randomly selected microscopic fields ($35\,200 \mu\text{m}^2/\text{field}$) of viable tissue at high power ($\times 400$); cell proliferation was quantitatively expressed as number per mm².

2.9 | Blood microvascular and lymphatic vessel densities, and lymphatic vessel invasion

CD31 and podoplanin (or LYVE-1) are markers for blood vessel endothelium and lymphatic endothelium, respectively. CD31-positive blood microvessels in primary tumor sections were enumerated as previously described.³² Briefly, the slides were scanned at low-power ($\times 100$) magnification to identify areas with the highest

number of CD31-positive vessels and 5 areas of the highest microvascular density were selected for quantitation under higher ($\times 200$ – 400) magnification.

To determine the lymphatic vessel density in primary tumors, we counted the number of podoplanin- or LYVE-1-positive lymphatic vessels in the whole tumor section and expressed as numbers per cm^2 . Although carcinoma cells were not entirely detected in the lumen of tumor blood vessels, dilated lymphatic vessels frequently contained migrating tumor cells within the lumina (lymphatic vessel invasion). To determine the number of lymphatic vessel invasion in primary tumors, we counted the number of podoplanin-positive lymphatic vessels containing intraluminal tumor cells in whole tumor sections and expressed as numbers per cm^2 .

As the lymph nodes and lungs were the organs with greater metastasis in the present model, and secondary invasion into blood vessels in these organs were possibly attributed to cancer spread, the number of blood vessels that contained intraluminal tumor cells were counted histopathologically using H&E-stained slides.

2.10 | Real-time RT-PCR analysis

We specifically microdissected only visible mammary carcinoma tissues from FFPE tumors using a laser microdissector (LMD7000; Leica Microsystems) as described previously,²⁷ to avoid including necrotic and mesenchymal tissues in real-time RT-PCR analysis. FFPE primary tumor tissues were analyzed using real-time RT-PCR.²⁷ Total RNA was extracted from FFPE tumor samples using the RNeasy FFPE Kit (Qiagen, GmbH) and cDNAs were synthesized using a Primer Script RT Reagent Kit with gDNA Eraser (Takara Bio). We subsequently amplified the resulting cDNAs using a Thermal Cycler Dice Real-time System (Takara Bio) and SYBR Premix Ex TaqII (TaKaRa Bio). Amplification cycles were as follows: an initial step at 95°C for 30 s, followed by 45 cycles of 5 s at 95°C , 10 s at 58°C , and 20 s at 72°C . The primer sequences are presented in Table 1. Relative gene expression was normalized to the housekeeping gene *Gapdh* (ΔC_t) and was calculated as fold change compared with controls using the $2^{-\Delta\Delta\text{C}_t}$ method.³³

Genes	Forward primer sequences (5'→3')	Reverse primer sequences (5'→3')
<i>Gapdh</i>	TGGCCTTCGGTGTTCCTACC	AGCCAAGATGCCCTTCAGT
<i>Vegfr1</i>	CTATCGGCTGTCCATGAAA	ATCCTCGGTTGTCACATCT
<i>Vegfr2</i>	TGATTTCACTGGCACTC	GTATTCCCCTTGGTCACTC
<i>Vegfr3</i>	GCATGTGCCAGTATTGT	ACGCTGCACAGATAACGAC
<i>Vegfa</i>	CACTGGACCTGGCTTTA	TCAATCGGACGGCAGTAG
<i>Vegfc</i>	AACGTGTCCAAGAAATCAG	TGGATCACAATGCTTCAGT
<i>Vegfd</i>	ACTTGGTGCAGGGCTTCAGG	CATCGCCACAGCTTCCAGTC
<i>Pcna</i>	TGGAGAGCTTGGCAATGG	CCTCAGAGCAAACGTTAGGTG
<i>Lyve1</i>	AAGCCTATTGCCACAACATC	TTGCGGGTGTGGAGTGTC
<i>Cd31</i>	GCCAACAGCCATTACGGTTA	GGACTTCCACTTCTGTGTATTC

TABLE 1 Mouse primer sequences for real-time PCR using FFPE samples

2.11 | Statistical analysis

Mann-Whitney *U*-test (an unpaired group and non-parametric analysis) was used to compare the quantitative data in the control and psVEGFR-3 groups. Student *t* test with the Welch method, which accounts for insufficient homogeneity of variance, was performed to analyze the quantitative data between the control and psVEGFR-3 groups. Data were expressed as mean \pm SD and differences were considered statistically significant for $P < .05$.

3 | RESULTS

3.1 | Study in vitro

Figure 1A shows that BJMC3879Luc2 cell growth was increased significantly by VEGF-C at >0.1 ng/mL, but diminished at 200 ng/mL. The maximum effective VEGF-C dose was 100 ng/mL. Subsequently, BJMC3879Luc2 cells were transfected with ps-VEGFR-3 or control (pVec) vectors with or without VEGF-C addition (100 ng/mL). The growth of BJMC3879Luc2 cells transfected with psVEGFR-3 was significantly decreased compared with pVec alone and significantly reduced in cells transfected with psVEGFR-3 and VEGF-C compared with pVec and VEGF-C (Figure 1B). In addition, the growth of cells significantly increased when transfected with pVec + VEGF-C compared with pVec alone (Figure 1B).

3.2 | Body weights and tumor growth

One mouse in the psVEGFR-3 group died at week 2 due to an accidental overdose of anesthetic during gene electrotransfer and was excluded from analysis. At weeks 5 and 6, 3 animals from the pVec group (control) died due to widespread metastasis of mammary carcinoma. As shown in Figure 2A, the body weights did not differ statistically between the groups throughout the experiment.

Primary tumor volumes are presented in Figure 2B. Compared with control mice, the tumor volumes suppressed significantly from weeks 2 through 6 in the psVEGFR-3 group.

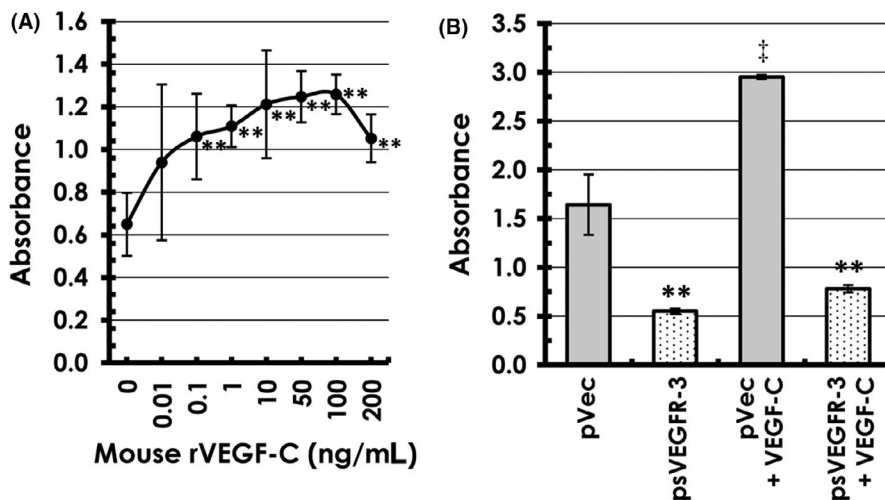
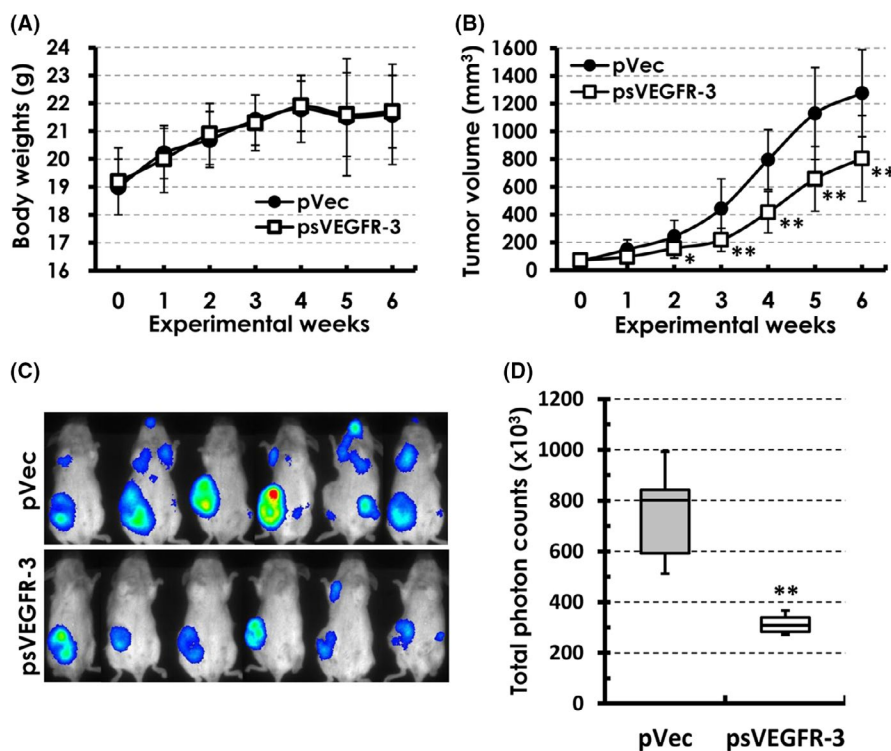


FIGURE 1 Proliferative activities of mammary carcinoma cells transfected with *sVefr3* gene and VEGF-C in vitro. A, Growth of BJMC3879Luc2 cells is significantly increased by >0.1 ng/mL, but depressed by 200 ng/mL. Maximum effective dose is 100 ng/mL. B, Cell growth is significantly diminished by transfection with psVEGFR-3 compared with pVec (control) and with psVEGFR-3 + 100 ng/mL VEGF-C compared with pVec + VEGF-C. In addition, cell growth is significantly increased by pVec + VEGF-C compared with pVec alone. Data represent means \pm SD. ** $P < .01$ compared with pVec or pVec + VEGF-C; † $P < .01$ compared with pVec

FIGURE 2 Body weights, primary mammary tumor volumes, and photon counts of the tumors in mice receiving intratumoral gene through control pVec or psVEGFR-3. A, Body weights were similar between groups throughout the study. B, From weeks 2-6, gains in tumor volumes were significantly suppressed in psVEGFR-3-treated mice versus pVec-treated controls. C, Bioluminescence imaging at week 6 in 6 representative mice from each group. D, Bioluminescence imaging indicated reduction in metastasis expansion in the sVEGFR-3 group compared to the control group. Data represent the mean \pm SD. * $P < .05$; ** $P < .01$



3.3 | Bioluminescent imaging

Bioluminescent imaging signals indicated metastatic growth in the mandibular, axillary, and inguinal lymphatic regions in both the control and therapeutic groups (Figure 2C). However, metastatic expansion mice from the psVEGFR-3 group was significantly lower compared with that in control animals (Figure 2D).

3.4 | Histopathological analysis

The primary mammary tumors induced by BJMC3879Luc2 cell inoculation uniformly appeared to be adenocarcinomas with infrequent glandular formation; we observed no histopathological differences among groups (data not shown). Figure 3A,B shows representative lymph node metastases. The number of metastasis-positive lymph

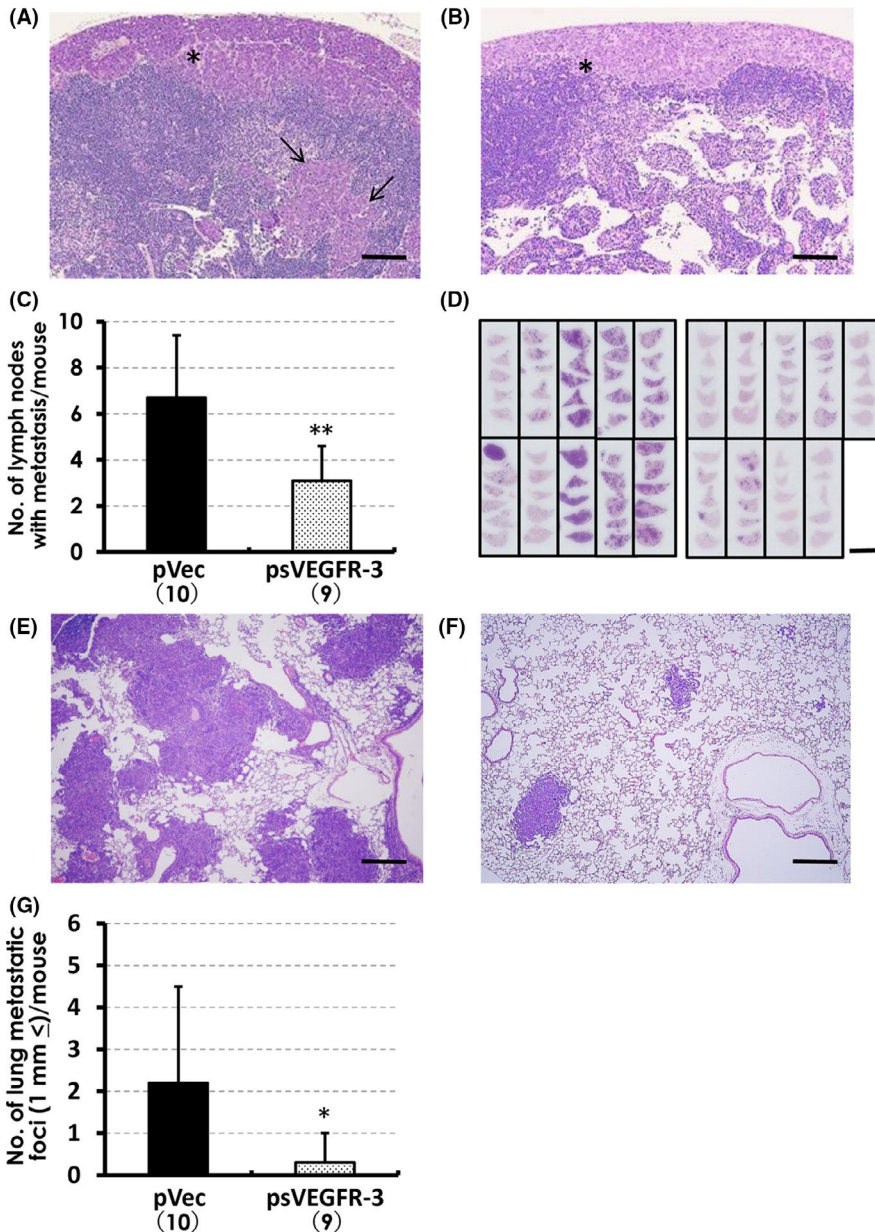


FIGURE 3 Metastasis to lymph nodes and lungs in mammary carcinomas. A, Metastasis to a lymph node in a control mouse. Metastatic carcinoma cells filled the subcapsular space (asterisk) and invaded into the sinusoid space (arrows). B, Lymph node from a mouse in the psVEGFR-3 group. Metastatic carcinoma cells were detected in the subcapsular sinus (asterisk) and were absent in the sinusoidal space. C, Multiplicity of lymph node metastasis is significantly reduced in the psVEGFR-3 group versus the control group. D, Macroscopic view of lung histopathology slides from all surviving mice after week 6 in the control and psVEGFR-3 groups. Metastatic foci are abundant in lungs from the control group (purple areas, left panel), but scarce in those from the psVEGFR-3 group (right panel). E, Metastatic foci in the lungs of a control mouse observed by light microscopy. Many metastatic foci and small to large nodules were observed. F, Metastatic foci in the lungs of a mouse in the psVEGFR-3 group. Metastatic foci were fewer and much smaller. G, Multiplicity of lung metastatic foci measuring ≥ 1 mm was significantly reduced in the psVEGFR-3 group. (A, B, D-F) H&E staining; Scale bars: (A, B, E, F) 100 μ m; (D) 1 cm. Data represent the mean \pm SD. * $P < .05$; ** $P < .01$. Numerals in parentheses indicate the number of animals examined

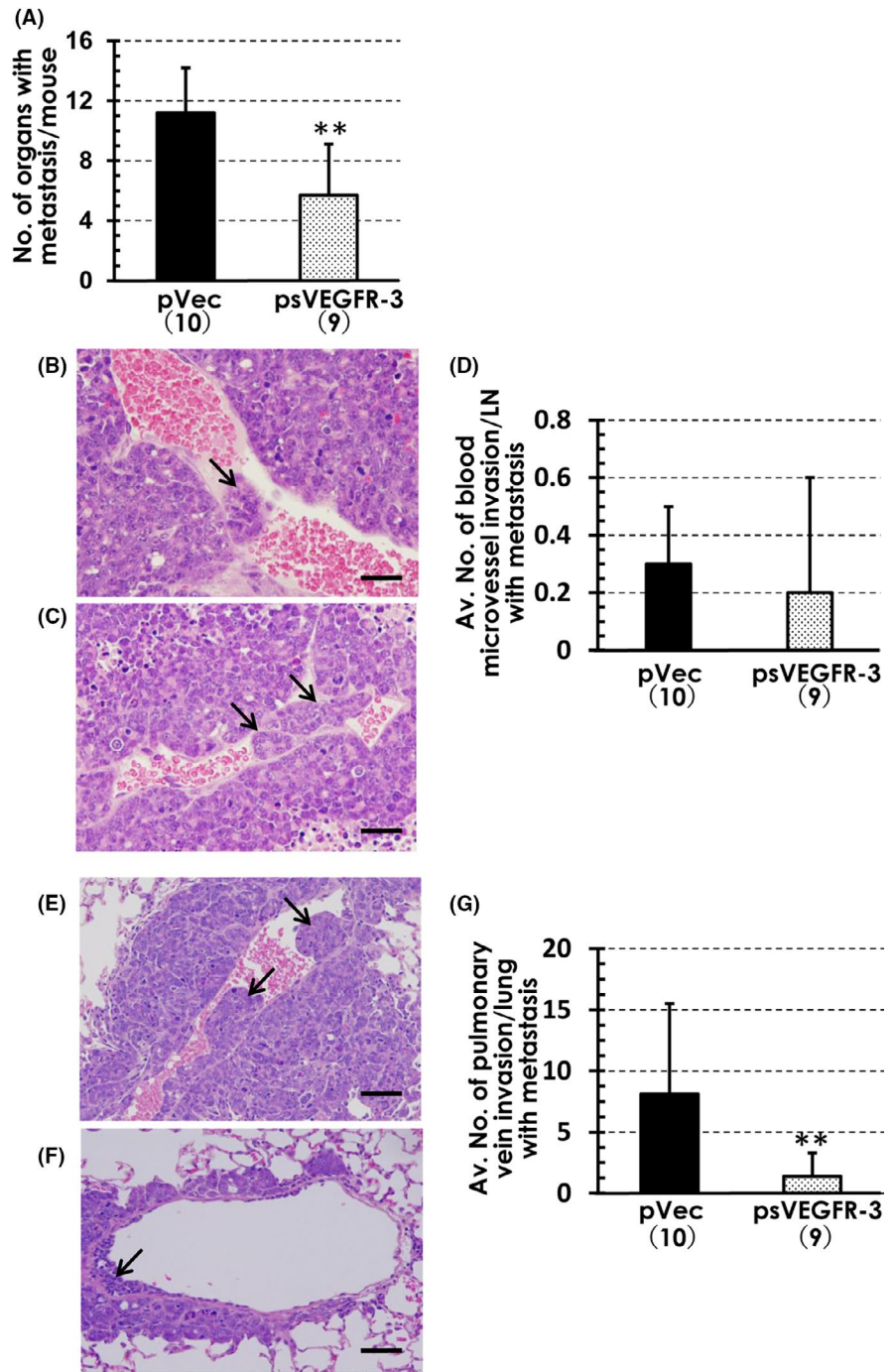
nodes per mouse was significantly reduced in the psVEGFR-3 group compared with the control group (Figure 3C).

The macroscopic view of histopathology lung slides from all animals indicated numerous larger metastatic foci in the control group (Figure 3D, left panel), and fewer and smaller foci were observed in the psVEGFR-3 group (Figure 3D, right panel). Metastatic lung foci were less abundant and smaller in the psVEGFR-3 group than the control group (Figure 3E,F). The multiplicity of the lung metastasis ≥ 1 mm per mouse was significantly reduced in the psVEGFR-3 group compared with that in the control group (Figure 3G).

Metastatic foci were observed in adrenals, ovaries, and kidneys as well. When evaluating the number of affected organs, unilateral metastasis in bilateral organs such as kidneys was counted as 1, and

bilateral metastases were counted as 2. The average number of all organs with metastasis per mouse was significantly lower in the psVEGFR-3 group compared with the control group (Figure 4A). In this model, lymph nodes and lungs were the organs with higher metastasis and secondary invasion into blood vessels in these organs is possibly attributed to spread of cancer. Cancer cells present in the lumen of the blood microvessels in the lymph nodes were observed in both the control (Figure 4B) and psVEGFR-3-treated groups (Figure 4C). The average number of blood microvessel invasions per metastatic lymph node was similar in both groups (Figure 4D). Although the pulmonary vein was frequently filled with cancer cells in both groups (Figure 4E,F), the average number of blood vessel invasions in the lungs was significantly lower in the psVEGFR-3 group than in the control group (Figure 4G).

FIGURE 4 Multi-organ metastasis and blood vessel invasion in lymph nodes and lungs A, Average number of organs with metastasis per mouse was significantly reduced in the psVEGFR-3 group. Blood microvessels in lymph nodes invaded by cancer cells (arrows) in a control mouse (B) and a mouse treated with psVEGFR-3 (C). D, Average numbers of invaded blood microvessels in lymph nodes are similar between groups. Pulmonary vein with invading cancer cells (arrows) in a control mouse (E) and a mouse treated with psVEGFR-3 (F). G, Average number of pulmonary vein invasions is significantly lower in the psVEGFR-3 group. (B, C, E, F) H&E staining; Scale bars: (B, C, E, F) 50 μ m. Data represent the mean \pm SD. ** $P < .01$. Numbers in parentheses indicate the number of animals examined



3.5 | Apoptosis and cell proliferation

Representative TUNEL-positive apoptotic cells in the primary mammary tumors are presented in Figure 5A,B. Results of quantitative analyses of apoptosis in mammary carcinomas are presented in Figure 5C. The number of TUNEL-positive cells in the pVec (control) and psVEGFR-3 groups were comparable (Figure 5C).

Cell proliferation in primary mammary carcinomas was examined using PCNA immunohistochemical analysis (Figure 5D,E). The PCNA-positive rates of the mammary tumor cells were significantly lower in the psVEGFR-3 group compared with that in the control group (Figure 5F).

3.6 | Blood microvascular and lymphatic vessel densities, and lymphatic vessel invasion

Blood microvascular density, as determined by immunohistochemical analysis of the blood vessel endothelial cell marker CD31 (Figure 6A,B), was comparable between the pVec (control) and psVEGFR-3 groups (Figure 6C).

Lymphatic vessel density, as determined by immunohistochemical analysis of the lymphatic vessel epithelial marker podoplanin or LYVE-1 (Figure 6D,E), was significantly lower in the psVEGFR-3 group compared to that in the control group (Figure 6F) (refer to Figure 9A for LYVE-1). Carcinoma cells detected within the lumina

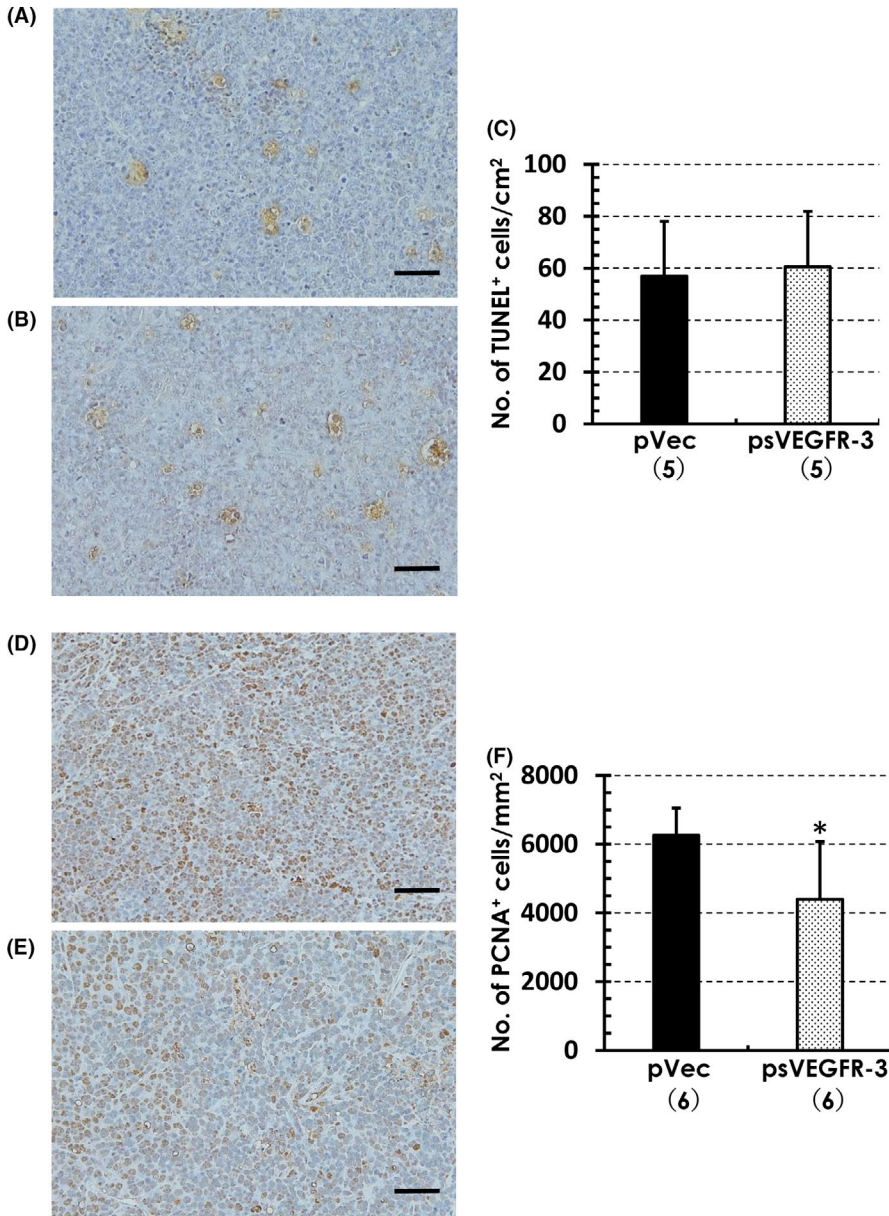


FIGURE 5 Apoptosis and cell proliferation in primary mammary carcinomas. Number of TUNEL-positive apoptotic cells was similar between the control (A) and the psVEGFR-3 (B) groups. Graphic representation of these data (C). Number of PCNA-positive cells was significantly lower in the psVEGFR-3 group (E) compared with the control group (D). Graphic representation of these data (F). A, B, TUNEL reaction; D, E, PCNA immunohistochemistry; Scale bars: (A, B, D, E) 50 μ m. Data represent the mean \pm SD. * $P < .05$. Numbers in parentheses indicate the number of animals examined

of dilated tumors lymphatic vessels in both control (Figure 6D) and psVEGFR-3-treated mice (Figure 6E) indicated lymphatic vessel invasion. However, as shown in Figure 6G, the average number of lymphatic vessel invasions was significantly reduced in the psVEGFR-3 group compared with the control group.

3.7 | Real-time RT-PCR analysis

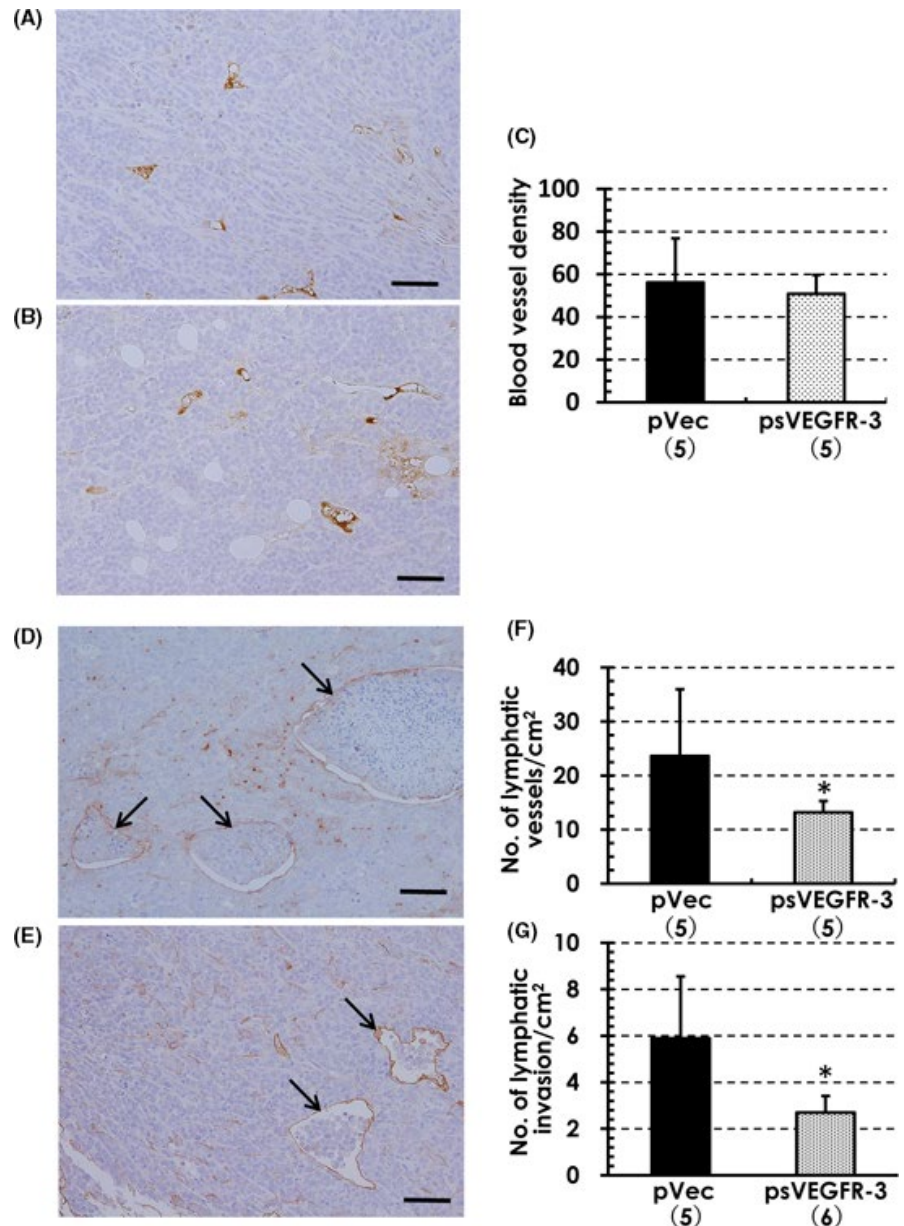
Real-time RT-PCR analysis was conducted using FFPE primary mammary carcinomas. Relative expression of the *Vegf* receptor (*Vegfr*) family is presented in Figure 7A. Significantly high levels of *Vegfr3* were observed in the psVEGFR-3 group and considered to result from the gene introduction from the psVEGFR-3 vector. There was no difference in *Vegfr1* and *Vegfr2* levels between the groups. There were no differences in the levels of *Vegfa*, *Vegfc*, and *Vegfd* between groups

(Figure 7B). Relative levels of *Pcna* and *Lyve1* tended to decrease in the psVEGFR-3 group; however, it was statistically insignificant (Figure 7C). Relative levels of *Cd31* were similar between groups (Figure 7C). The data on *Pcna*, *Lyve1*, and *Cd31* closely corresponded with the immunohistochemical findings (refer to Figure 9A for LYVE-1).

3.8 | Tyrosine phosphorylation and LYVE-1⁺ lymphatic vessels

Immunofluorescence staining for detecting tyrosine phosphorylation indicated that p-Tyr expression was lower in tumor cells from psVEGFR-3-treated mammary carcinomas than in those from pVec-treated mammary carcinomas (Figure 8A,B). As indicated in Figure 9A, a significant reduction in LYVE-1⁺ lymphatic vessels was observed in psVEGFR-3-treated mammary carcinomas compared

FIGURE 6 Angiogenesis, lymphangiogenesis, and lymphatic vessel invasion in mammary carcinomas. Number of CD31-positive blood endothelial cells was similar between the control (A) and the psVEGFR-3 (B) groups. Graphical representation of these data (C). Number of podoplanin-positive lymphatic endothelial cells (D, E) was significantly reduced in the psVEGFR-3 group. Graphic representation of these data (F) (also refer to Figure 9A). Podoplanin-positive lymphatic vessels of mammary tumors were often dilated and filled with carcinoma cells (arrows, D, E), indicative of lymphatic vessel invasion. The number of lymphatic vessel invasions was significantly lower in the psVEGFR-3 group than in the control pVec group. Graphical representation of these data (G). A, B, CD31 immunohistochemistry; (D, E) Podoplanin immunohistochemistry; (A, B, D, E) Scale bars: 50 μ m. Data represent the mean \pm SD. * $P < .05$. Numbers in parentheses indicate the number of animals examined



with pVec-treated mammary carcinomas (Figure 8C,D). Tyrosine phosphorylation in lymphatic vessels (arrows; p-Tyr⁺/LYVE-1⁺ in Figure 8E-H) tended to reduce in primary mammary carcinomas from psVEGFR-3-treated mice (Figure 8F,H) compared with those from pVec-treated mice (Figure 8E,G; graphically shown in Figure 9B).

4 | DISCUSSION

The present study showed that *sVegfr3* gene therapy suppressed multi-organ metastasis in a mouse model of metastatic mammary cancer. The inhibition of primary tumor growth and metastasis was associated with reduction in cell proliferation, lymphatic vessel density, lymphatic vessel invasion, and tyrosine phosphorylation in tumor lymphatic vessels. In fact, psVEGFR-3 significantly diminished cell growth with or without VEGF-C addition in vitro. These findings

are attributed to a blockade of VEGFR-3/VEGF-C signaling as a result of sVEGFR-3 binding to VEGF-C.

Human breast cancers primarily metastasize to lymph nodes, lungs, liver, and bone, and such extensive and intractable metastasis leads to death. Tumor size and nodal status are practical parameters for prognosis estimation.³⁴ Once breast cancer tumors reach a diameter of ≥ 4 cm, the chances of tumor recurrence and/or metastasis significantly increases.³⁴ Therefore, *sVegfr3* gene therapy that can suppress both tumor growth and multi-organ metastasis would have significant clinical implications. Furthermore, lymph node metastasis is one of the worst negative prognostic factors for patients with breast cancer.³⁵ The significant reduction in the overall numbers of organ metastases involving lymph nodes substantiates the effectiveness of *sVegfr3* gene therapy.

Dissemination of cancer cells can occur in different modes, such as in local tissue invasion and/or migration via blood and lymphatic

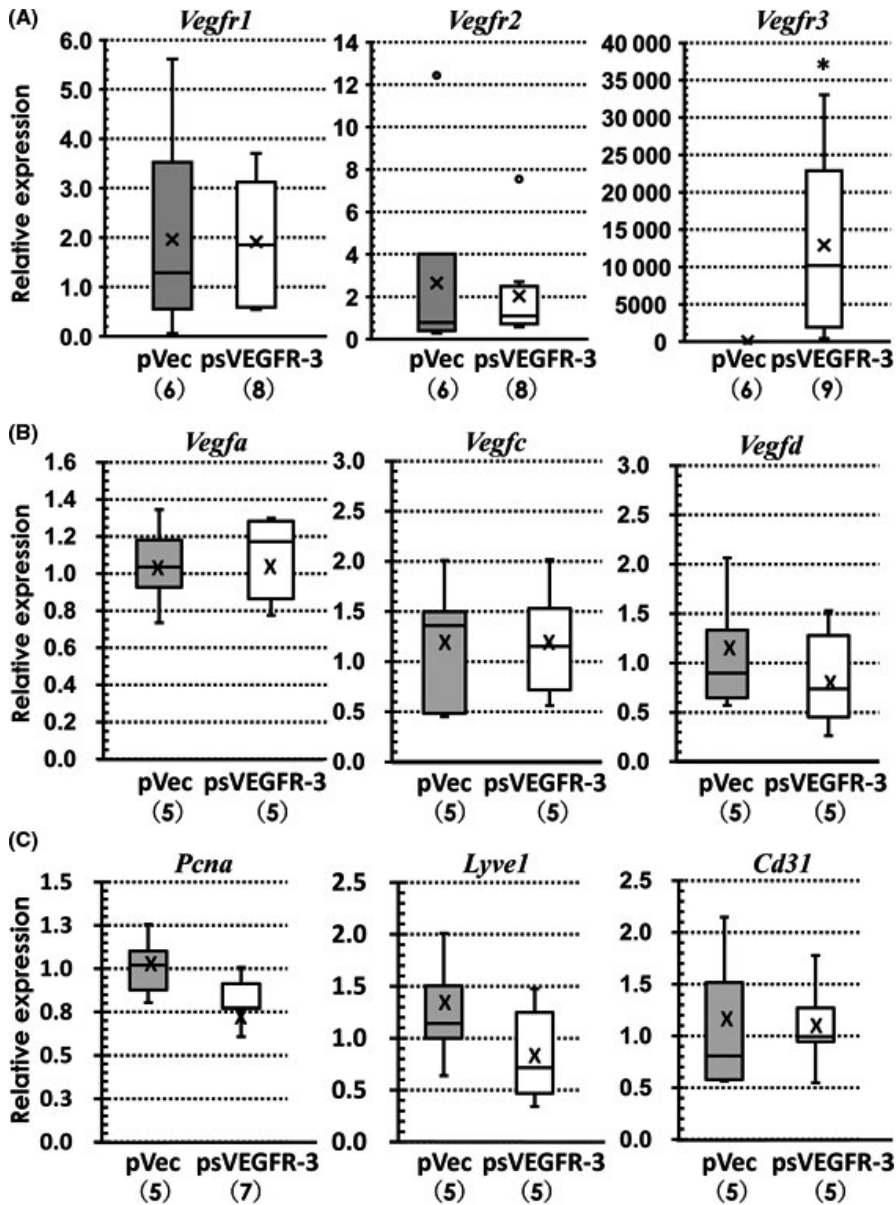


FIGURE 7 Real-time RT-PCR analyses of formalin-fixed paraffin-embedded (FFPE) mammary carcinomas. A, In the *Vegfr* family, there were no apparent differences in *Vegfr1* and *Vegfr2* levels between groups. Although *Vegfr3* levels were significantly elevated in the psVEGFR-3 group (* $P < .05$), this was due to the introduction of the *Vegfr3* gene. B, In the *Vegf* family, relative levels of *Vegfa*, *Vegfc*, and *Vegfd* were similar between groups. C, Levels of *Pcnal* and *Lyve1* tended to reduce in the psVEGFR-3 group, however the differences were statistically insignificant. *Cd31* levels were similar between groups. Numbers in parentheses indicate the number of animals examined. The boxes represent the 25th to 75th percentiles; horizontal lines within the box represent median values and X indicates mean values. The whiskers extend either to the 10th or 90th percentiles, respectively

vessels. The most common pathway of the initial dissemination of several solid malignancies occurs through the lymphatics, and lymph nodes act as bridgeheads of metastatic spread.³⁶ Malignant cells move into the bloodstream to reach distant sites as well, with subsequent lymph/blood crossover events. Mammary cancer preferentially metastasized to the lymph nodes and lungs of our model mice. We frequently observed cancer cells in the lumen of the pulmonary vein in the lungs, and the number of blood vessel invasions in the lung was significantly lower in the psVEGFR-3 group. This indicated that *sVegfr3* inhibited secondary cancer spread and helped to suppress multi-organ metastasis. Alternatively, sVEGFR-3 secreted into the bloodstream might bind and sequesters circulating VEGF-C, thus inhibiting the settlement of cancer cells in metastatic organs. Notably, significantly decreased amounts of sVEGFR-3 in the bloodstream correlate with lung cancer patients.³⁷ Blood vessel invasion was observed in the metastatic lymph nodes as well, however there was no difference between the groups.

VEGF-C overexpression correlates with lymph node metastasis in a variety of human neoplasms, including breast cancers.^{38,39} Several studies in animal models have demonstrated that VEGF-C accelerates tumor lymphangiogenesis and leads to metastatic spread of tumor cells to lymph nodes and distant organ metastasis.¹³ Therefore, tumor cell-derived VEGF-C enhances lymph node metastasis. Conversely, downregulation of VEGF-C with siRNA inhibits tumor growth²⁰⁻²² and lymph node metastasis.^{19,20,40}

VEGFR-3, the VEGF-C receptor, is frequently expressed in lymphatic endothelial cells,⁴¹ and the VEGF-C-dependent activation of VEGFR-3 induces lymphangiogenesis driven by the keratin 14 promoter in the skin of transgenic mice,⁴² while disruption of VEGFR-3 signaling by receptor mutations results in lymphatic hypoplasia.⁴³ In addition, inhibition of VEGFR-3 activation by blocking antibodies suppresses lymph node metastasis in animal models of cancer and is associated with a reduction in tumor lymphangiogenesis.^{17,18,44} Furthermore, blocking of VEGFR-3 signaling by sVEGFR-3 reduced

FIGURE 8 Tyrosine phosphorylation in mammary carcinoma cells and tumor lymphatic vessels. Membranous expression of p-Tyr in cancer cells was strong in mammary tumors from a control mouse (A), while the expression was lower in a mouse treated with psVEGFR-3 (B). The number of LYVE-1⁺ lymphatic vessels was much lesser in a mouse receiving psVEGFR-3 (D) than in a control mouse (C) (refer to Figure 9A; a significant reduction of the number in the psVEGFR-3 group). p-Tyr⁺/LYVE-1⁺ (arrows in E and F) demonstrate a decreasing trend in mouse receiving psVEGFR-3 (F) compared with that in a control mouse (E). (G, H) represent higher magnification of an inset in (E) and (F), respectively. A, B, p-Tyr immunofluorescence staining; (C, D) LYVE-1 immunofluorescence staining; (E-H) Merged images of p-Tyr (A, B), LYVE-1 (C, D) and DAPI nuclear staining. (G, H) Higher magnification of (E) and (F), respectively. Scale bars: (A-F) 100 μ m; (G, H) 200 μ m

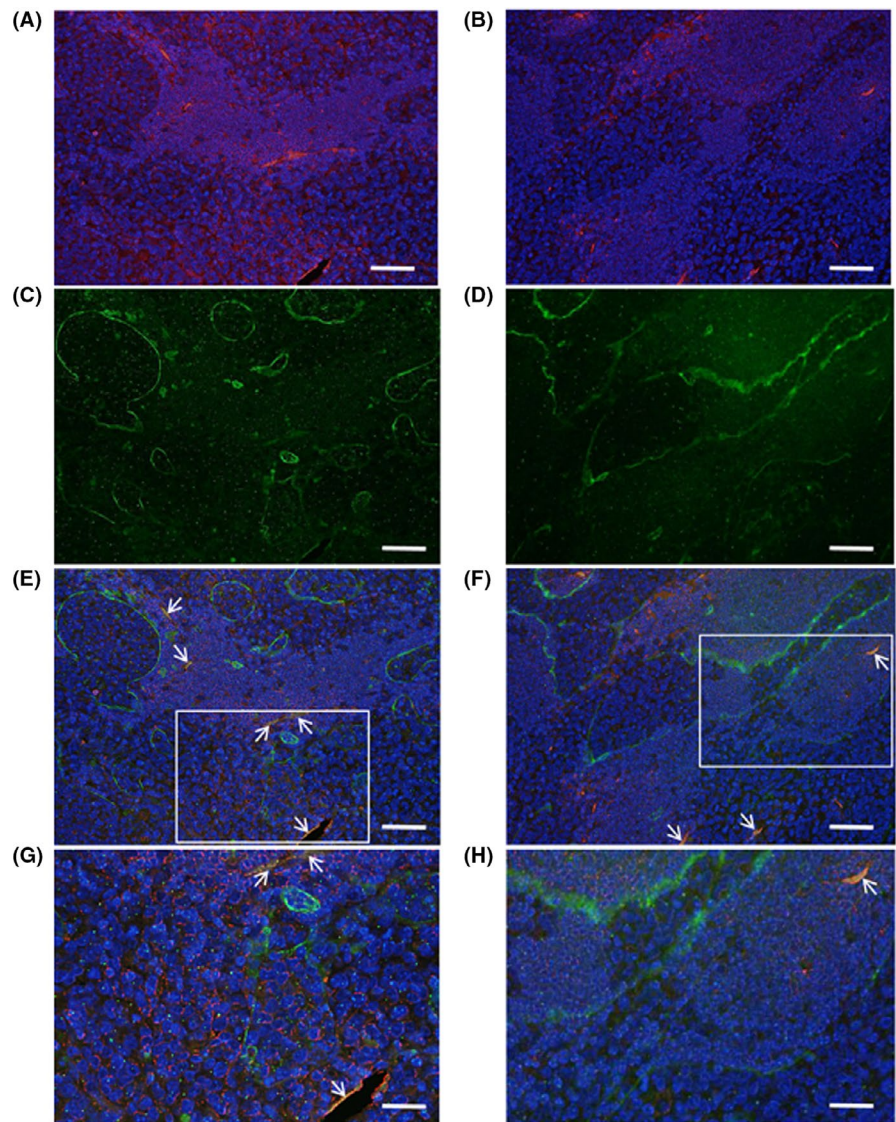
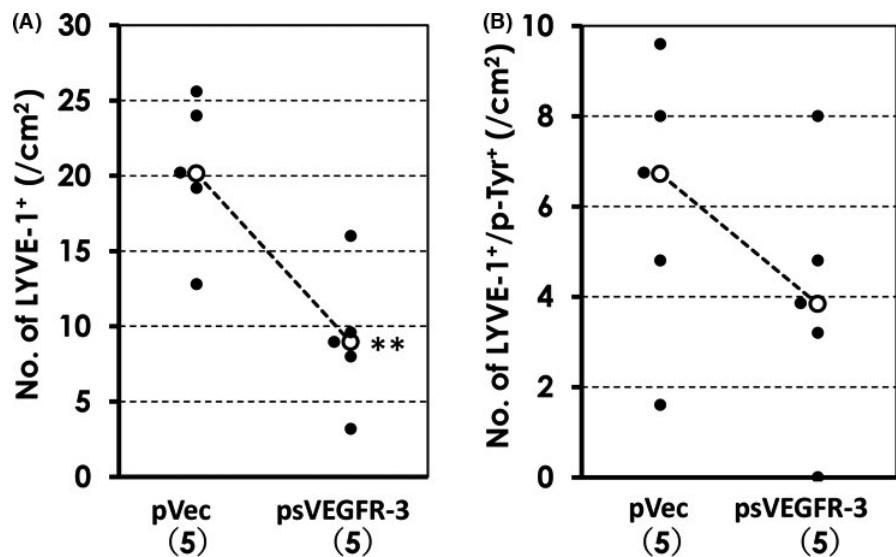


FIGURE 9 Quantitative analysis of lymphatic vessels and tyrosine phosphorylation in mammary carcinoma lymphatic vessels. A, Number of LYVE-1⁺ lymphatic vessels was significantly lower in the psVEGFR-3 group compared with that in the control group. B, While the number of LYVE-1⁺/p-Tyr⁺ tended to reduce in the psVEGFR-3 group, it was statistically insignificant. A, B, Scatter plot diagram (white circle indicates mean). ** $P < .01$. Numbers in parentheses indicate the number of animals examined



lymphangiogenesis and lymph node metastasis,²³⁻²⁵ while angiogenesis was unaffected.²³ Therefore, newly formed lymphatic capillaries, as well as preexisting afferent lymphatic vessels, served as a route for the dissemination of tumor cells during lymph node metastasis.^{6,10,11,45} Additionally, this study revealed that sVEGFR-3 significantly reduced lymphangiogenesis while angiogenesis remained unaffected. sVEGFR-2, an endogenous soluble isoform of the VEGF-C receptor, was reported to function as a specific inhibitor of lymphatic vessel growth,⁴⁶ a subsequent study revealed that sVEGFR-2 suppressed tumor growth and lymph node metastasis in a mouse mammary model specifically through inhibition of lymphangiogenesis by sequestering VEGF-C, while it did not affect angiogenesis.²⁶ As VEGF-A maintains blood vessel integrity, prolonged systemic administration of anti-VEGF-A agents in cancer is accompanied by side-effects (due to lack of normal VEGF functioning) such as increased risk of arterial hypertension and embolism.⁴⁷ It influences the survival of blood vessels in healthy tissues⁴⁸ as well. Therefore, sVEGFR-3 therapy may prevent side-effects through anti-angiogenesis.

Expression of VEGFR-3 in cancer cells has been reported in human breast cancer tissues^{49,50} as well, indicating that VEGFR-3 overexpression enhances breast cancer cell proliferation, motility, and survival.⁴⁹ Furthermore, recent studies have revealed that VEGFR-3 expression is detected in various types of cancers and contributes to tumor progression and lymphatic metastasis.⁵¹ These findings indicated that VEGF-C/VEGFR-3 signaling participates in different types of cancers linked with mammary cancer. In this connection, VEGFR-3 expression in the BJMC3879 mouse mammary carcinoma cell line used in this study is detected by western blots³⁰ as well.

Tyrosine kinases in the lymphatic endothelium are involved in processes such as maintenance of existing lymphatic vessels, growth and maturation of new vessels, and function.⁵² VEGFR-3, a tyrosine kinase receptor, is activated by its ligand VEGF-C that results in phosphorylation of tyrosine residues.¹³ Tyrosine phosphorylation is also known to regulate receptor kinase activity and signal transduction in cancer cells.^{13,53} Therefore, VEGFR-3 is an attractive target for cancer therapy that delays cancer progression. In the present study, expression of p-Tyr in mammary cancer cells was reduced in the sVEGFR-3 group compared with that in the control pVec group as observed through immunofluorescence staining. As reliable anti-mouse VEGFR-3 phosphorylation antibodies for FFPE section are commercially unavailable, we conducted double immunofluorescence staining with p-Tyr and LYVE-1 to detect tyrosine phosphorylation in tumor lymphatic vessels. The number of p-Tyr⁺/LYVE-1⁺ vessels tended to be reduced in tumors treated with psVEGFR-3 compared with the control. In addition, primary tumors contained significantly fewer LYVE-1⁺ lymphatic vessels in the sVEGFR-3 group. These findings indicate that *sVegfr3* therapy influenced VEGF-C/VEGFR-3 signaling.

In conclusion, *sVegfr3* gene therapy significantly suppressed multi-organ metastasis and several parameters of tumor metastasis in a mouse model of mammary cancer. Our findings have prognostic significance for human cancers in terms of the development of novel clinical therapeutic methods for treating of human metastatic diseases.

ACKNOWLEDGMENTS

This study was funded by the Japan Society for the Promotion of Science, Grant/Award Number: 21591682 (MA Shibata). We thank Ms Himika Kashiwai for her laboratory assistance and Ms Kaoru Okimoto for her secretarial assistance.

CONFLICT OF INTEREST

The authors have no conflict of interest to declare.

ORCID

Masa-Aki Shibata  <https://orcid.org/0000-0002-3350-7305>

REFERENCES

1. World Health Organization. Cancer in Fact sheets. Fact sheets updated December 2018. <http://www.who.int/news-room/fact-sheets/detail/cancer>. Accessed April 28, 2020.
2. Agarwal G, Pradeep PV, Aggarwal V Yip CH, Cheung PS. Spectrum of breast cancer in Asian women. *World J Surg*. 2007;31:1031-1040.
3. Brinton LA, Sherman ME, Carreon JD, Anderson WF. Recent trends in breast cancer among younger women in the United States. *J Natl Cancer Inst*. 2008;100:1643-1648.
4. Nguyen DX, Massague J. Genetic determinants of cancer metastasis. *Nat Rev Genet*. 2007;8:341-352.
5. Shibuya M. Vascular endothelial growth factor and its receptor system: physiological functions in angiogenesis and pathological roles in various diseases. *J Biochem*. 2013;153:13-19.
6. Alitalo K, Carmeliet P. Molecular mechanisms of lymphangiogenesis in health and disease. *Cancer Cell*. 2002;1:219-227.
7. Achen MG, Stacker SA. Molecular control of lymphatic metastasis. *Ann NY Acad Sci*. 2008;1131:225-234.
8. Joukov V, Pajusola K, Kaipainen A, et al. A novel vascular endothelial growth factor, VEGF-C, is a ligand for the Flt4 (VEGFR-3) and KDR (VEGFR-2) receptor tyrosine kinases. *EMBO J*. 1996;15:290-298.
9. Achen MG, Jeltsch M, Kukk E, et al. Vascular endothelial growth factor D (VEGF-D) is a ligand for the tyrosine kinases VEGF receptor 2 (Flk1) and VEGF receptor 3 (Flt4). *Proc Natl Acad Sci USA*. 1998;95:548-553.
10. Skobe M, Hawighorst T, Jackson DG, et al. Induction of tumor lymphangiogenesis by VEGF-C promotes breast cancer metastasis. *Nat Med*. 2001;7:192-198.
11. Mandriota SJ, Jussila L, Jeltsch M, et al. Vascular endothelial growth factor-C-mediated lymphangiogenesis promotes tumour metastasis. *EMBO J*. 2001;20:672-682.
12. Karpanen T, Egeblad M, Karkkainen MJ, et al. Vascular endothelial growth factor C promotes tumor lymphangiogenesis and intralymphatic tumor growth. *Cancer Res*. 2001;61:1786-1790.
13. Achen MG, Mann GB, Stacker SA. Targeting lymphangiogenesis to prevent tumour metastasis. *Br J Cancer*. 2006;94:1355-1360.
14. Mylona E, Alexandrou P, Mpakali A, et al. Clinicopathological and prognostic significance of vascular endothelial growth factors (VEGF)-C and -D and VEGF receptor 3 in invasive breast carcinoma. *Eur J Surg Oncol*. 2007;33:294-300.
15. Nakamura Y, Yasuoka H, Tsujimoto M, et al. Lymph vessel density correlates with nodal status, VEGF-C expression, and prognosis in breast cancer. *Breast Cancer Res Treat*. 2005;91:125-132.
16. Zhao YC, Ni XJ, Li Y, et al. Peritumoral lymphangiogenesis induced by vascular endothelial growth factor C and D promotes lymph node metastasis in breast cancer patients. *World J Surg Oncol*. 2012;10:165.
17. Shimizu K, Kubo H, Yamaguchi K, et al. Suppression of VEGFR-3 signaling inhibits lymph node metastasis in gastric cancer. *Cancer Sci*. 2004;95:328-333.

18. Roberts N, Kloos B, Cassella M, et al. Inhibition of VEGFR-3 activation with the antagonistic antibody more potently suppresses lymph node and distant metastases than inactivation of VEGFR-2. *Cancer Res.* 2006;66:2650-2657.
19. Chen Z, Varney ML, Backora MW, et al. Down-regulation of vascular endothelial cell growth factor-C expression using small interfering RNA vectors in mammary tumors inhibits tumor lymphangiogenesis and spontaneous metastasis and enhances survival. *Cancer Res.* 2005;65:9004-9011.
20. Shibata MA, Morimoto J, Shibata E, Otsuki Y. Combination therapy with short interfering RNA vectors against VEGF-C and VEGF-A suppresses lymph node and lung metastasis in a mouse immunocompetent mammary cancer model. *Cancer Gene Ther.* 2008;15:776-786.
21. Shi Y, Tong M, Wu Y, et al. VEGF-C ShRNA inhibits pancreatic cancer growth and lymphangiogenesis in an orthotopic fluorescent nude mouse model. *Anticancer Res.* 2013;33:409-417.
22. Yao J, Da M, Guo T, Duan Y, Zhang Y. RNAi-mediated gene silencing of vascular endothelial growth factor-C inhibits tumor lymphangiogenesis and growth of gastric cancer in vivo in mice. *Tumour Biol.* 2013;34:1493-1501.
23. Lin JM, Lalani AS, Harding TC, et al. Inhibition of lymphogenous metastasis using adeno-associated virus-mediated gene transfer of a soluble VEGFR-3 decoy receptor. *Cancer Res.* 2005;65:6901-6909.
24. Yang H, Kim C, Kim MJ, et al. Soluble vascular endothelial growth factor receptor-3 suppresses lymphangiogenesis and lymphatic metastasis in bladder cancer. *Mol Cancer.* 2011;10:36.
25. Takahashi K, Mizukami H, Saga Y, et al. Suppression of lymph node and lung metastases of endometrial cancer by muscle-mediated expression of soluble vascular endothelial growth factor receptor-3. *Cancer Sci.* 2013;104:1107-1111.
26. Shibata MA, Ambati J, Shibata E, et al. The endogenous soluble VEGF receptor-2 isoform suppresses lymph node metastasis in a mouse immunocompetent mammary cancer model. *BMC Med.* 2010;8:69.
27. Shibata MA, Hamaoka H, Morimoto J, et al. Synthetic α -mangostin dilaurate strongly suppresses wide-spectrum organ metastasis in a mouse model of mammary cancer. *Cancer Sci.* 2018;109:1660-1671.
28. Shibata MA, Morimoto J, Otsuki Y. Suppression of murine mammary carcinoma growth and metastasis by HSVtk/GCV gene therapy using *in vivo* electroporation. *Cancer Gene Ther.* 2002;9:16-27.
29. Shibata MA, Shibata E, Morimoto J, et al. An immunocompetent murine model of metastatic mammary cancer accessible to bioluminescence imaging. *Anticancer Res.* 2009;29:4389-4396.
30. Shibata MA, Ito Y, Morimoto J, Kusakabe K, Yoshinaka R, Otsuki Y. *In vivo* electrogene transfer of interleukin-12 inhibits tumor growth and lymph node and lung metastases in mouse mammary carcinomas. *J Gene Med.* 2006;8:335-352.
31. Shibata MA, Liu M-L, Knudson MC, et al. Haploid loss of *bax* leads to accelerated mammary tumor development in C3(1)/SV40-TAG transgenic mice: reduction in protective apoptotic response at the preneoplastic stage. *EMBO J.* 1999;18:2692-2701.
32. Gorrin-Rivas MJ, Arii S, Furutani M, et al. Mouse macrophage metalloelastase gene transfer into a murine melanoma suppresses primary tumor growth by halting angiogenesis. *Clin Cancer Res.* 2000;6:1647-1654.
33. Livak KJ, Schmittgen TD. Analysis of relative gene expression data using real-time quantitative PCR and the $2^{-\Delta\Delta C(T)}$ Method. *Methods.* 2001;25:402-408.
34. Carter CL, Allen C, Henson DE. Relation of tumor size, lymph node status, and survival in 24,740 breast cancer cases. *Cancer.* 1989;63:181-187.
35. Cody HS III, Borgen PI, Tan LK. Redefining prognosis in node-negative breast cancer: can sentinel lymph node biopsy raise the threshold for systemic adjuvant therapy? *Ann Surg Oncol.* 2004;11:227S-230S.
36. Sleeman JP. The lymph node as a bridgehead in the metastatic dissemination of tumors. *Recent Results Cancer Res.* 2000;157:55-81.
37. Addison CL, Ding K, Seymour L, et al. Analysis of serum protein levels of angiogenic factors and their soluble receptors as markers of response to cediranib in the NCIC CTG BR.24 clinical trial. *Lung Cancer.* 2015;90:288-295.
38. Salven P, Lymboussaki A, Heikkilä P, et al. Vascular endothelial growth factors VEGF-B and VEGF-C are expressed in human tumors. *Am J Pathol.* 1998;153:103-108.
39. Valtola R, Salven P, Heikkilä P, et al. VEGFR-3 and its ligand VEGF-C are associated with angiogenesis in breast cancer. *Am J Pathol.* 1999;154:1381-1390.
40. Shibata MA, Shibata E, Morimoto J, Harada-Shiba M. Therapy with siRNA for *Vegf-c* but not for *Vegf-d* suppresses wide-spectrum organ metastasis in an immunocompetent model of metastatic mammary cancer. *Anticancer Res.* 2013;33:4237-4247.
41. Kaipainen A, Korhonen J, Mustonen T, et al. Expression of the *fms*-like tyrosine kinase 4 gene becomes restricted to lymphatic endothelium during development. *Proc Natl Acad Sci USA.* 1995;92:3566-3570.
42. Veikkola T, Jussila L, Mäkinen T, et al. Signalling via vascular endothelial growth factor receptor-3 is sufficient for lymphangiogenesis in transgenic mice. *EMBO J.* 2001;20:1223-1231.
43. Karkkainen MJ, Ferrell RE, Lawrence EC, et al. Missense mutations interfere with VEGFR-3 signalling in primary lymphoedema. *Nat Genet.* 2000;25:153-159.
44. He Y, Kozaki K, Karpanen T, et al. Suppression of tumor lymphangiogenesis and lymph node metastasis by blocking vascular endothelial growth factor receptor 3 signaling. *J Natl Cancer Inst.* 2002;94:819-825.
45. Stacker SA, Baldwin ME, Achen MG. The role of tumor lymphangiogenesis in metastatic spread. *Faseb J.* 2002;16:922-934.
46. Albuquerque RJC, Hayashi T, Cho WG, et al. Alternatively spliced vascular endothelial growth factor receptor-2 is an essential endogenous inhibitor of lymphatic vessel growth. *Nat Med.* 2009;15:1023-1030.
47. Porta M, Striglia E. Intravitreal anti-VEGF agents and cardiovascular risk. *Intern Emerg Med.* 2019.
48. Olsson AK, Dimberg A, Kreuger J, Claesson-Welsh L. VEGF receptor signalling – in control of vascular function. *Nat Rev Mol Cell Biol.* 2006;7:359-371.
49. Kurenova EV, Hunt DL, He D, et al. Vascular endothelial growth factor receptor-3 promotes breast cancer cell proliferation, motility and survival in vitro and tumor formation in vivo. *Cell Cycle.* 2009;8:2266-2280.
50. Baker E, Whiteoak N, Hall L, France J, Wilson D, Bhaskar P. Mammaglobin-A, VEGFR3, and Ki67 in human breast cancer pathology and five years survival. *Breast Cancer (Auckl).* 2019;13:1178223419858957.
51. Hsu MC, Pan MR, Hung WC. Two birds, one stone: double hits on tumor growth and lymphangiogenesis by targeting vascular endothelial growth factor receptor 3. *Cells.* 2019;8(3):270.
52. Williams SP, Karnezis T, Achen MG, Stacker SA. Targeting lymphatic vessel functions through tyrosine kinases. *J Angiogenesis Res.* 2010;2:13.
53. Chang Y-W, Su C-M, Su Y-H, et al. Novel peptides suppress VEGFR-3 activity and antagonize VEGFR-3-mediated oncogenic effects. *Oncotarget.* 2014;5:3823-3835.

How to cite this article: Shibata M-A, Shibata E, Tanaka Y, Shiraoka C, Kondo Y. Soluble *Vegfr3* gene therapy suppresses multi-organ metastasis in a mouse mammary cancer model. *Cancer Sci.* 2020;111:2837-2849. <https://doi.org/10.1111/cas.14531>